December 2017

Effects of Sodium Chloride on Anthracene Photolysis Kinetics in Aqueous-Organic Solutions

Kyle Blaha
Syracuse University

Abstract

Polycyclic aromatic hydrocarbons (PAHs) are dangerous pollutants. The photolysis kinetics of PAHs are of interest because they are carcinogenic and can increase in toxicity through photodegradation into secondary products. They are often associated with particulate matter. The composition and physical properties of the particulate matter can affect PAH photolysis kinetics. We investigated the effects of sodium chloride on the photolysis kinetics of the PAH anthracene in water and octanol as well as mixed-phase solutions (water-octanol), which were used as models for aqueous-organic aerosols. A non-linear dependence on sodium chloride concentrations was observed. Sodium chloride enhanced photolysis at concentrations up to 0.25 M due to increased singlet oxygen ($^1O_2$) production, and suppressed photolysis at higher concentrations because of anthracene quenching. A positive dependence on sodium chloride concentration above sodium chloride's saturation limit in aqueous solution (6.1 M) suggested that new reaction pathways, potentially on the surface of solid sodium chloride, may be occurring. 0.25 M sodium chloride increased rate constants in octanol and aqueous-organic mixtures, but to a lesser extent than in water. An increase of a factor of 9 was observed when 0.25 M sodium chloride was included in aqueous solutions, while the increase in octanol was a factor of 2. Stirring aqueous-organic mixtures during photolysis increased photolysis rates in the absence of salt, but had inconsistent effects in the presence of 0.25 M sodium chloride.

EFFECTS OF SODIUM CHLORIDE ON ANTHRACENE PHOTOLYSIS KINETICS IN AQUEOUS-ORGANIC SOLUTIONS

by

Kyle Blaha

B.A., Hiram College, 2015

Thesis

Submitted in partial fulfillment of the requirements for the degree of

Master of Science in *chemistry*.

Syracuse University

December 2017

Acknowledgements

Many thanks to my thesis advisor, Dr. Tara Kahan, for her advisement and support the past two and a half years. She was an excellent leader and helped me become a better scientist and academic. Her numerous suggestions, tips, and editing were essential to my success.

Lab members Shawn Kowal, Alexa Stathis, Annastacia Stubbs, Corey Kroptavich, and Shan Zhou for their support with the everyday work activities. They were paramount in helping me understand key concepts and were always eager to lend a helping hand.

Prior lab members Jarod Grossman and Phil Malley for their prior work that inspired many of the topics researched. Thanks for their expertise and training when I was first starting my project and for their continued support throughout the remainder of their time in the lab.

NSF-NRT EMPOWER Program leads, Deanna McCay and Laura Lautz; their interest and support was a key source of motivation. Their absolute excellence in creating a scientific community on campus through the program was remarkable.

For financial support, I thank Dr. Tara Kahan, the NSF-NRT EMPOWER program, and the Chemistry Department at Syracuse University.

Contents

Table of Figures

1 - Introduction

1.1 - Aerosols

1.1.1 - Classification and Formation

An aerosol is a particle that is suspended in air or gas. Aerosols can be liquid or solid, can be a large variety of shapes and sizes, and can originate from vastly different processes. Atmospheric aerosols affect climate, atmospheric composition, and human health. The chemical processes, such as the reaction with sunlight, that occur within aerosols create a vast array of secondary products. The composition of aerosols, in many cases including volatile organic compounds, can have adverse health effects which can be enhanced through photochemical reactions by creating toxic products. Therefore, it is important to understand the chemical processes that occur within aerosols.

There are two major classes of atmospheric aerosols: primary aerosols and secondary aerosols. A primary aerosol is directly emitted to the atmosphere. There are a handful of processes that can cause this, such as wind and wave-breaking action. The burning of fossil fuels also generates primary aerosols. The typical diameter of primary aerosols is greater than 2.5 µm; these large aerosols are often referred to as coarse particles (Finlayson-Pitts and Pitts Jr 2000). Particles larger than 10 µm in diameter tend to not survive long in the atmosphere due to their sedimentation velocities (Jacob 1999).

Wave-breaking action in the ocean creates sea-salt aerosols, one of the most abundant types of aerosols in the atmosphere, particularly in or near marine environments (Finlayson-Pitts and Pitts Jr 2000). Breaking waves caused by winds that trap air under the surface of the water forms bubbles that burst at the surface, ejecting particles into the atmosphere (George

et al. 2015). It has also been shown that wave-breaking action of freshwater can create aerosols in a way that is mechanistically similar (May et al. 2016).

Beyond the breaking of waves, the burning of fuels is another source of coarse aerosol production. Black carbon is produced by combustion of carbon (Simoneit 2002). Studies have shown that black carbon is one of the most common particles formed from the burning of fossil fuels (George et al. 2015).

Mineral dust is another large source of particulate matter in the atmosphere, particularly in arid regions. Wind action ejects between 1,500-2,000 Tg of dust into the atmosphere each year (George et al. 2015). Other common coarse-mode particulate matter includes pollen, fungal spores, and cloud droplets (George et al. 2015).

Secondary aerosols are created by reactions of gases in the atmosphere, and mostly consist of sulfates, nitrates, and organics (Hallquist et al. 2009). Gas molecules undergo nucleation to produce ultra-fine particles. These particles are typically less than 0.01 µm in diameter and rapidly grow through condensation and coagulation. This process produces fine particles, with diameters of 0.01 µm to 1 µm (Jacob 1999). Nucleation of sulfuric acid is one of the more common sources of secondary aerosols (Finlayson-Pitts and Pitts Jr 2000). In this process sulfur dioxide (SO_2) is emitted from combustion into the atmosphere and is oxidized into sulfuric acid (H_2SO_4). H_2SO_4 nucleates to form aqueous sulfate particles because of its low vapor pressure. Low vapor pressure gases, such as ammonia, nitric acid, and organic species can then condense onto the sulfate particles (Hallquist et al. 2009). The atmospheric oxidation

of volatile organic compounds in the gas phase and subsequent condensation onto existing particles creates organic-rich particulate matter in the atmosphere.

Secondary aerosols tend to not grow much past 1 µm due to the slow rate of condensation. Aerosols that form from condensation accumulate in the atmosphere. The size of atmospheric aerosols, as well as its composition, determines how long they can exist. Atmospheric aerosols in urban air can be present for several hours before undergoing deposition or being transported out, while they can survive for days in rural air until removal from the atmosphere; fine aerosols in the troposphere can potentially exist for weeks before complete removal from the atmosphere (Finlayson-Pitts and Pitts Jr 2000). Environmental processes such as rainfall or acting as nuclei for cloud droplet formation can remove aerosols (Jacob 1999).

Aerosols can contain either aqueous or organic components, or a mixture of both. If the mixture is immiscible, then it has been shown that a phase-separated structure is likely to be formed as seen in the cartoon representation in Figure 1. Water in the atmosphere almost always has an organic outer film (Donaldson and Vaida 2006). Organic films can act as a barrier that prevents transfer of gases into the solution, but can also serve as a different solution phase to which hydrophobic molecules can partition (Donaldson and Vaida 2006).

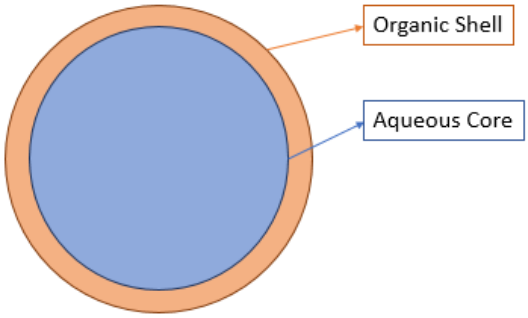

Figure 1: Side-view of a core-shell aerosol. The organic shell surrounds the aqueous core.

A study has shown that the ability for a core-shell structure to form in an aerosol is much greater if the components of the aerosol have large solubility differences in water. It also showed that core-shell structures with organic layers happen more frequently than it had been previously believed; an organic component in an aqueous aerosol is more likely to form an immiscible solution as opposed to a miscible solution (Freedman et al. 2010).

1.1.2 - Effects of Aerosols

Aerosols have both direct and indirect effects on the climate. They directly affect climate by scattering and absorbing solar radiation. Solar radiation is scattered by an aerosol when the light's path is disrupted. Scattering can be reflection, refraction, or diffraction (Finlayson-Pitts and Pitts Jr 2000). Most scattering of solar radiation by particles in the atmosphere is done by fine particles (Larson and Cass 1989). Sulfates injected into the stratosphere, particularly from volcanic eruptions, are effective at scattering solar radiation (Jacob 1999). Indirect effects of aerosols on climate stem from their ability to serve as the nuclei for cloud formation. Clouds and fogs can scatter solar radiation efficiently (Finlayson-Pitts and Pitts Jr 2000). The amount of radiation reflected into space by clouds can result in a cooling of Earth's surface temperatures (Jacob 1999).

Another effect that aerosols can have is lowering visibility. Visibility in urban areas is significantly less than in areas less polluted by aerosols (Jacob 1999). The measure of total light scattered and absorbed for airborne particles is the extinction coefficient. The extinction coefficient in urban areas, particularly during the summer-time, is large. This can equate to a visual range of just 1-3 km in a large city such as Los Angeles during historically polluted times (Larson and Cass 1989). For comparison, the human eye would have a visual range of up to 300 km in an atmosphere devoid of aerosols (Jacob 1999).

Aerosols can cause a myriad of health issues in humans. Aerosols are a danger for the respiratory and cardiovascular systems. It has been reported that premature deaths arise from aerosol exposure, with the World Health Organization (WHO) reporting an estimated 3.7 million people in 2012 alone (WHO 2015). Particulate matter smaller than 2.5 μm ($PM_{2.5}$) exist longer in the atmosphere compared to larger particulate matter. This small particulate matter is particularly dangerous because it can be inhaled into the lungs and can end up in the bloodstream. Many of the organic components of $PM_{2.5}$ can be mutagenic. The high level of toxicity of the organic components has not been widely studied due to its complexity (Turpin et al. 2000). $PM_{2.5}$ is primarily created through the burning of organic carbon, notably vehicle emission (Turpin et al. 2000).

$PM_{2.5}$ contain chemicals capable of generating reactive oxygen species (ROS) in the lungs. ROS can be damaging to several internal body systems. This includes the ability of ROS to damage DNA and cause amino acid oxidation (Shiraiwa et al. 2012). ROS damage in the body has been linked to cancers, Alzheimer's, and asthma (Jung et al. 2014). While ROS do have a

positive use in the body, such as cell signaling, the damage they can cause in excess can pose a health hazard.

Soot, or black carbon, is another health hazard within aerosols. Breathing in black carbon can result in an array of respiratory issues. Many of the organic molecules in soot, such as polycyclic aromatic hydrocarbons (PAHs), are known carcinogens (George et al. 2015). Organic pollutants like these, created from combustion, are in heavier concentrations in urban areas, creating a larger health risk.

1.2 - Polycyclic Aromatic Hydrocarbons

1.2.1 - Overview and Sources

PAHs are organic molecules consisting of coupled aromatic rings. They are produced through incomplete combustion of carbon. While they can be natural, anthropogenic sources such as vehicle emissions are the primary source (Yunker et al. 2002). Due to the nature of their production they are a key component of many primary aerosols. Studies have shown a significant health risk from PAHs largely stemming from them being carcinogenic (Bostrom et al. 2002).

Despite being a high-profile pollutant, estimates for PAH in particulate matter are more uncertain than other common pollutants (Turpin et al. 2000). This is because of less-developed methodology for measurement and less frequent measurements than with other pollutants. Key contributors of PAH are automobile exhaust, wood burning, and production of coal tar and asphalt (Bostrom et al. 2002).

Another key source of PAH emissions into the atmosphere is from industry and energy production. Production of coal and oil are large sources, as well as manufacturing plants

focused on aluminum and rubber. Residential heating, furnaces, and ovens also contribute to PAH emissions, sometimes in quantities higher than vehicle emissions (Yunker et al. 2002). In the United States and Sweden, wood burning to heat homes is reported to be the largest PAH source in rural areas, where wood-heated homes are more prevalent than in urban areas (Bostrom et al. 2002). It has been shown that PAH levels are higher in the winter as opposed to the summer, because of urban heating and reduced photochemical processes (Pirjola et al. 2017). Natural sources of PAH in the atmosphere stem mainly from forest fires and oil seepage (Yunker et al. 2002).

The PAH that was studied in this work was anthracene ($C_{14}H_{10}$). Anthracene consists of three fused benzene rings as seen in Figure 2. Anthracene is a dangerous contaminant that often can be found in water and aerosols.

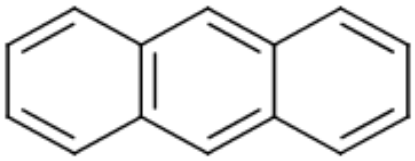

Figure 2: Molecular structure of Anthracene ($C_{14}H_{10}$)

Anthracene is the second most emitted PAH from vehicle emissions, behind only phenanthrene (Yan et al. 2014). Beyond combustion sources, anthracene is used in protective coatings for construction projects that keep drainage pipes waterproof and corrosion resistant. For similar reasons, it can be found in coatings of road paving, cement and bricks. While the

concentrations are not particularly high within asphalt coatings (around 1.6 ppt) as the coating degrades and washes away, the anthracene can enter and contaminate water sources (Irwin 1997).

Typical anthracene concentrations in drinking water are between 1.1 and 59.7 ppt (Irwin 1997). Higher concentrations of anthracene in water are found in industrial areas. One study showed that concentrations of anthracene in water samples taken from wood treatment sites in Canada have particularly high values, ranging from 15 ppb to 360 ppb (Irwin 1997). Anthracene concentrations in soil water around gas processing plants have been reported of up to 2.2 ppm (Irwin 1997). The EPA's water quality standard of anthracene in water for human health is 300 ppb (EPA 2015).

1.2.2 - Health Effects

PAHs are widely studied because they are carcinogenic and mutagenic. Carcinogenesis involves mutations at the cellular level, specifically the formation of tumors. PAHs can easily convert into electrophilic intermediates that readily bind with DNA, RNA, and proteins. PAH also interfere with the transcription receptor Ah, associated with cell growth and differentiation. PAHs have also been shown to block intercellular communication (Bostrom et al. 2002).

There are other health risks associated with PAHs. Some studies measured PAH exposure in children and observed a range of different negative health effects depending on the environment the children were raised in. PAH exposure has also been linked to asthma in children (Jung et al. 2014).

Human health is not the only reason to focus on PAHs. It has damaging effects on the ecosystems it is present in. A study showed that anthracene at concentrations of 12 ppb are toxic to bluegill populations after just nine hours of exposure (Irwin 1997). Anthracene can also be damaging to animals (Bostrom et al. 2002).

The photolysis of PAHs in aerosols under atmospheric conditions is a source of oxygenated aromatics, which can also be toxic and mutagenic. While photochemistry in the atmosphere will remove much of the parent PAH molecule, the products in its place can be just as dangerous. One study looked at phenanthrene and its major photooxidation product, 9,10-phenanthrenequinone. It found that the toxicity of the secondary organic compound was five times higher than the toxicity of the parent PAH (McConkey et al. 1997).

1.2.3 - Photolysis

Photolysis is chemical decomposition caused by light or other electromagnetic radiation. It is the core aging process of particles in the atmosphere (George et al. 2015). Organic pollutants in the atmosphere, such as PAHs, are broken down by these photochemical processes (Haritash and Kaushik 2009). Direct photolysis, where photons directly affect the molecule they interact with, can occur in particulate matter in the atmosphere (Finlayson-Pitts and Pitts Jr 2000). Indirect photolysis occurs when a molecule other than the analyte absorbs a photon and induces a reaction in the analyte through photosensitization or the production of reactive species. An example is reactions of PAHs with photochemically-formed hydroxyl radicals (OH) (Finlayson-Pitts and Pitts Jr 2000).

PAHs in the atmosphere exist in particulate matter, specifically $PM_{2.5}$ (Alves et al. 2017). Due to the abundance of particulate matter in the atmosphere as well as the adverse health

effects of PAHs, it is necessary to understand how quickly PAHs will photochemically react. The photodegradation rate of PAHs is dependent on the components included in aqueous solution. It was observed that a handful of photochemical processes were in play with PAH photolysis, including hydrogen abstraction and singlet oxygen reactions (McDow et al. 1996). Another study demonstrated the key role that O_2 plays in photochemical reactions. As O_2 concentrations increased, the quantum yields of PAH loss increased (Fasnacht and Blough 2003). Benzo[a]pyrene photolysis was nearly a factor of three faster in the presence of chrysene, but was slower in the presence of fluorene. It was thought that this could be due to the reactions between PAHs and oxidizing agents created by their excited states (Miller and Olejnik 2001).

Photolysis kinetics of PAHs in natural waters and pure waters are essentially the same (de Bruyn et al. 2012, Fasnacht et al. 2002). It was suggested that dissolved organic matter in natural waters does not significantly affect the photochemical rates (de Bruyn et al. 2012). In most studies done on PAHs in water, the studies assume that photolysis in pure water is representative of photolysis in nature.

While photolysis kinetics in natural and pure waters are essentially the same, the local environment can play a role. Anthracene photolysis was shown to be six times faster at ice surfaces compared to in liquid water (Kahan and Donaldson 2007). Like Fasnacht et al, this study illustrated that molecular oxygen plays a role in photodegradation, its presence increasing anthracene's photolysis rates on the ice surface more than in water. PAH photolysis on the surface of soil is also faster than in water (Xu et al. 2013).

Studies have shown that photolysis with aqueous and organic phased solutions can react differently depending on whether the solution is miscible or immiscible. PAHs are able to partition readily to the surface films, allowing them to potentially react different than PAHs in homogenous aerosols (Donaldson and Vaida 2006). Grossman showed that the average PAH photolysis rates in pure octanol were within error of experiments done in aqueous-organic mixtures containing less than 18%-volume water. It can be assumed that in a core-shell aerosol, with PAHs partitioned in the organic shell, the photochemistry of the PAHs is no different than it would be in a homogenous aerosol. In experiments with greater aqueous fractions, the rate constant increased (Grossman et al. 2016).

1.3 - Halides

Halides, such as sodium chloride in sea salt, can affect photolysis kinetics. As stated earlier, sea-salt aerosols are the most prevalent in the atmosphere. Wind action at the ocean surface, as well as wave-breaking action, generates sea-salt aerosols which contain Cl^- and Br^- (Keene et al. 2007) . Wind stress is the major source of reactive chlorine and bromine in marine air. The reaction of Cl^- at the surface of sea-salt aerosols is a main source of chlorine production in the marine boundary layer, the layer of the atmosphere in direct contact with the ocean surface (Spicer et al. 1998).

Particulate Cl^- and Br^- in acidic aerosols participate in atmospheric processes that generate Br_2 and Cl_2. Br_2 and Cl_2 volatize and photolyze to produce atomic Cl and Br, which are responsible for destruction of ozone (Keene et al. 2007). They catalytically destroy ozone in the troposphere, and halogen nitrates accelerate the creation of particulate NO_3^-, which contributes to total ozone destruction (Pszenny et al. 2004).

Recent work from our group showed that anthracene photolysis rate constants nearly tripled when sea water concentrations of sodium chloride were incorporated into aqueous solution. Halides did not affect pyrene photolysis kinetics (Grossman et al. in prep). Phenanthrene photolysis kinetics have also been reported not to depend on halides (de Bruyn et al. 2012).

1.4 - Statement of Need

In the past, people have investigated the effects of organic matter and halides on PAH photolysis kinetics separately, but not in combination. While these studies help determine what could be happening in nature, the many components would exist in an aerosol together in reality. The focus of this work was determining how sodium chloride affects anthracene photolysis kinetics in phase-separated aqueous-organic solutions. The effect halides might have on PAH in immiscible, core-shell aerosols has not been studied, and it is important to better understand the photolysis kinetics due to the adverse effects that PAHs can have on human health.

2 - Methods

2.1 - Materials

Saturated solutions (3×10^{-7} M) consisting of anthracene (Acros Organics, 99%) in 18.2 MΩ·cm deionized water were prepared every three weeks (Grossman et al. 2016). In a 100 mL vial, around 1 mg anthracene was mixed with 100mL water over night to create the saturated solutions. Solutions of anthracene in octanol (Acros Organics, 99%) were prepared every three weeks. 1.78 mg of anthracene was measured into 100 mL of octanol, creating 1.0×10^{-4} M anthracene. A series of dilutions was done to create the final experimental solution containing 1.0×10^{-7} M anthracene in octanol. Solutions were prepared two hours in advance and stirred

until the experiment began to ensure complete mixing. There was no statistical difference between solutions prepared two hours in advance and solutions stirred overnight.

Solutions were prepared using varying ratios of octanol and water to create mixed aqueous-organic solutions consisting of 50% or 90% octanol. For turbulent experiments, they were mixed for two hours prior to beginning the experiment to allow the layers to effectively mix. For stagnant experiments, they sat undisturbed for two hours prior to beginning the experiment. In the experiments where preparation involved a two-hour waiting period, the solutions were covered to prevent photolysis from fluorescent lighting in the lab space.

Sodium chloride (NaCl, Sigma-Aldrich, $\geq$99.5%) was incorporated into some solutions. In the aqueous experiments, sodium chloride concentrations ranged from 0.20 M to 10 M. In organic and aqueous organic experiments, sodium chloride concentrations ranged from 0.025 M to 1 M.

2.2 - Photolysis of Anthracene

Experiments all followed the same protocol. All experiments were run a minimum of three times. 4 mL of prepared anthracene solution was transferred via pipet to a quartz cuvette. This was covered until the time of the experiment. An initial fluorescence spectrum was acquired using a Photon Technology International Quantum Master 40 fluorimeter. Photolysis was performed in a 1 cm path length quartz cuvette unless otherwise noted. Samples were irradiated with the output of a 150 W xenon arc lamp that passed through a 295 nm long-pass cutoff filter, represented by the schematic in Figure 3. An IR filter was used to ensure that the sample was not heated during the experiment. The distance between the lamp and the sample was ~60 cm.

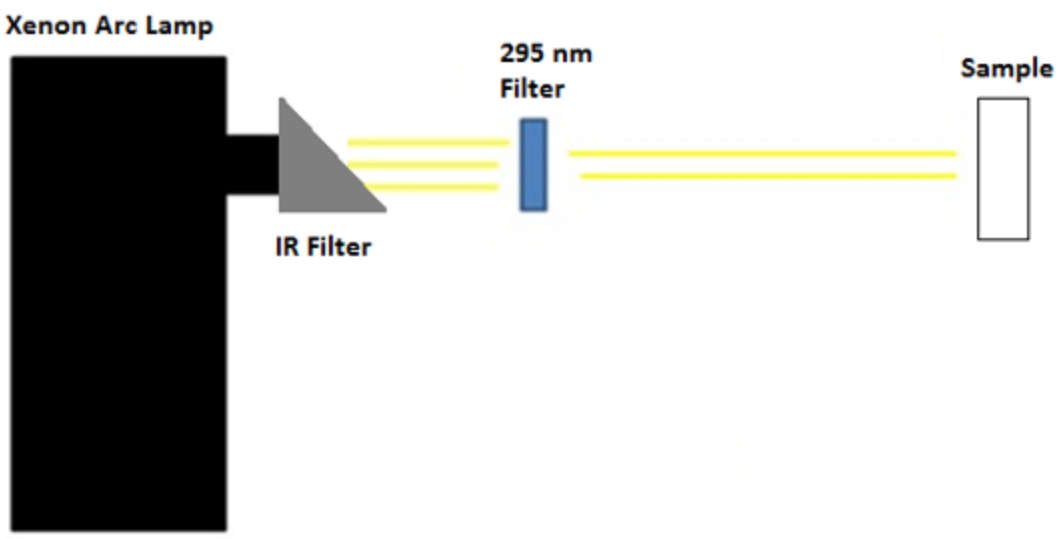

Figure 3: Instrument schematic showing light beam from xenon arc lamp irradiating sample

After an initial intensity reading was performed, the cuvette containing the anthracene solution was placed in front of the xenon arc lamp and in the middle of the beam spot. The solution was left in front of the lamp for a known time interval, at which point the sample was removed from the light and placed in the fluorimeter to acquire a second intensity reading. This was repeated at least 4 times to generate, at the very least, 5 intensity readings over time. Table 2 in the Appendix shows the time interval for each experimental configuration.

"Dark runs" were performed for anthracene in water solutions. The experimental procedure was identical to that for photolysis experiments except that the sample was shielded from the light. No change in fluorescence intensity over time was observed in these experiments.

Excitation spectra of anthracene were taken to determine which wavelength would be best suited as an excitation wavelength for fluorescence spectra. The largest peak found at 252

nm, seen in Figure 4, was shown to be the best wavelength suited for the excitation of anthracene due to it having the highest intensity.

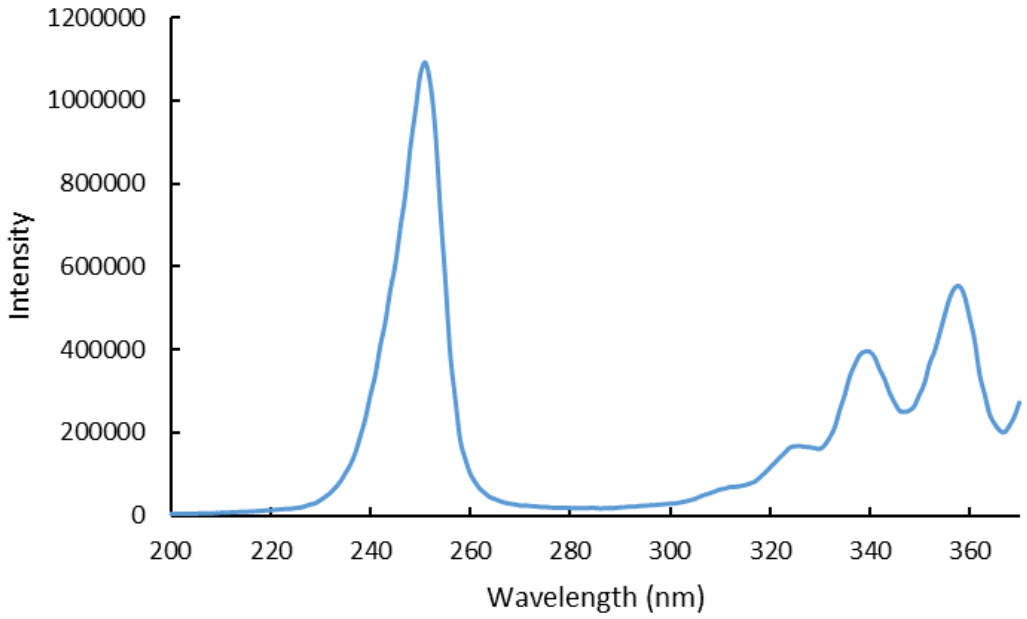

Figure 4: Excitation spectra of anthracene acquired with 380nm emission wavelength.

The emission wavelength range monitored was 360 nm to 460 nm. The slit widths, which control the amount of light reaching the sample in the fluorimeter, were set to 3.00 nm for the path entrance and 4.00 nm for the path exit for all experiments unless otherwise stated.

2.3 - Photolysis of Anthracene in Mixed Aqueous-Organic Solution

4 mL solutions were prepared and stirred with a micro stir-bar for 2 hours prior to the experiment time for mixed aqueous-organic experiments. For 50% octanol experiments, 2 mL of prepared anthracene in octanol solution was mixed with 2 mL deionized water as well as the desired amount of sodium chloride. For 90% octanol experiments, 3.6 mL of prepared anthracene in octanol solution was mixed with 0.4 mL deionized water as well as the desired amount of sodium chloride.

The experimental solution was placed into a quartz bowl to allow better mixing of the solution. The lamp apparatus was adjusted to accommodate the usage of the quartz bowl by installing a mirror that reflected the lamp down on the solution from above, in order to give the solution maximum exposure. After the experimental time interval, the solution in the quartz bowl was transferred via pipet into a cuvette, which was then placed in the fluorimeter for an intensity reading. The solution was transferred back to the quartz bowl after the reading and the procedure was repeated similar to prior experiments.

In mixed aqueous-organic solutions, the experiments were either done with the solution being constantly stirred during photolysis, or with them being stagnant during photolysis. For the experiments involving constant stirring, a 6 mm stir-bar was placed in the quartz bowl containing solution. In both the stagnant and the turbulent experiments, the solution was stirred while the fluorimeter was taking an intensity reading to mix the immiscible aqueous and organic phases.

2.4 - Data Analysis

Experimental data was analyzed in Microsoft Excel. For each photolysis experiment, calculations were done to determine the first and second order rate constant. Anthracene fluorescence intensity at 380 nm was plotted against irradiation time.

The first order rate constant was calculated using Equation 1, where I is the intensity at a given time, I_o is the initial intensity, k is the rate constant, and t is time. The natural log of intensity at time x divided by intensity at time zero was plotted vs. the time (in seconds) and a best fit line was applied. The slope of the line produced the first order rate constant. The second order rate constant was calculated using Equation 2. The intensity data was plotted vs.

time (in seconds) and the slope of the best fit line provided the second order rate constant. In all experiments performed, it was determined that the reaction was first order because it produced a more linear slope, as determined by the R^2 value of the best fit line.

$$\ln \frac{I}{I_o} = -kt \quad (1)$$

$$\frac{1}{I} = \frac{1}{I_o} + kt \quad (2)$$

3 - Results and Discussion

3.1 - Anthracene in Water

The photolysis kinetics of anthracene in deionized water have been measured in several previous studies. The rate constants measured in this work ($1.9\times10^{-4} \pm 1\times10^{-5}$ s^{-1}) was similar to previous measurements ($2.3\times10^{-4} \pm 2\times10^{-5}$ s^{-1}) (Grossman et al. 2016). Figure 5 demonstrates data from a typical anthracene photolysis experiment. A full table of anthracene photolysis data can be found in Table 2 in the Appendix. Figure 5 shows the first order photolysis of anthracene in 0.25 M sodium chloride plotted with the first order dark run of anthracene in the same solution. It was determined that the degradation rate of anthracene in the dark run was negligible; dark loss therefore did not likely contribute to measured anthracene photolysis rate constants in these experiments.

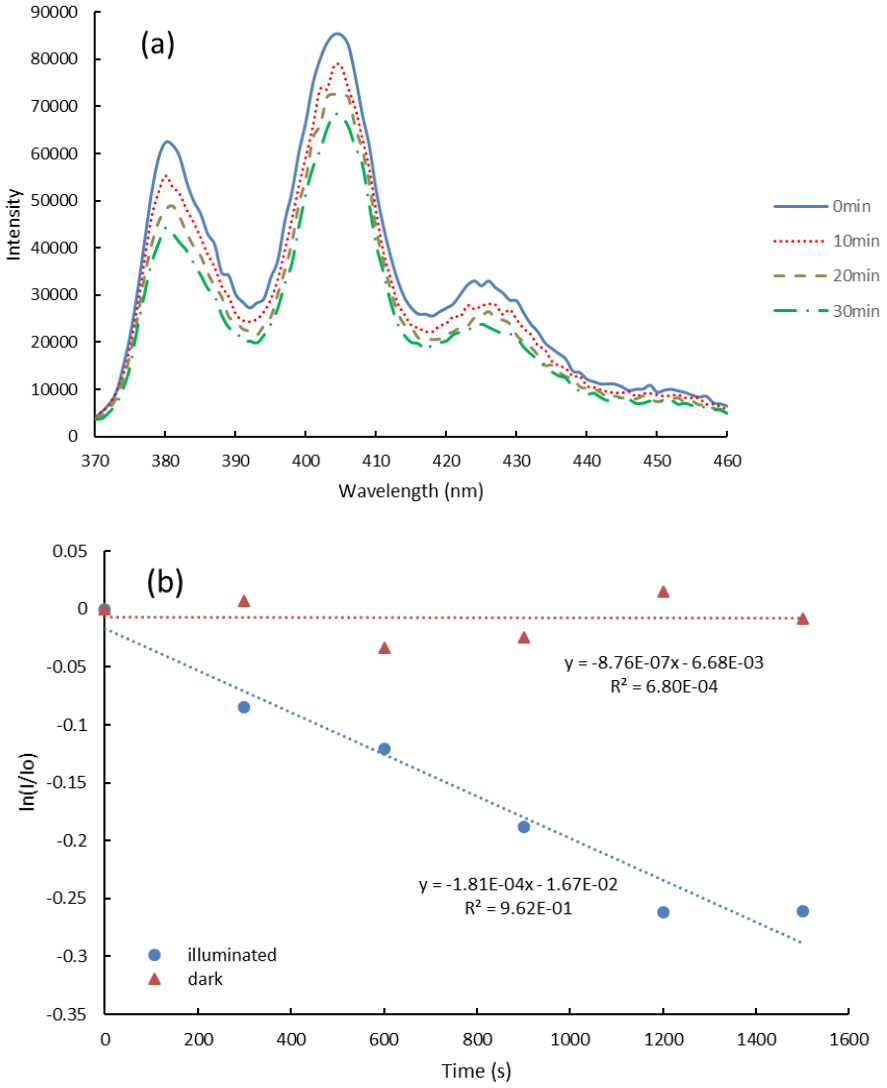

Figure 5: a) Anthracene emission spectra in water at various irradiation times. b) Anthracene emission intensity as a function of time in the dark and under illumination. The dotted traces are linear fits to the data.

3.2 - Effect of Sodium Chloride on Anthracene Photolysis

Figure 6 shows anthracene photolysis rate constants as a function of sodium chloride concentration in deionized water. The maximum in the rate constant at ~0.25 M sodium chloride has been observed in previous work from in this group (Grossman et al. in prep). The

current study extends the sodium chloride concentrations to values greater than the saturation limit in water (6.1 M).

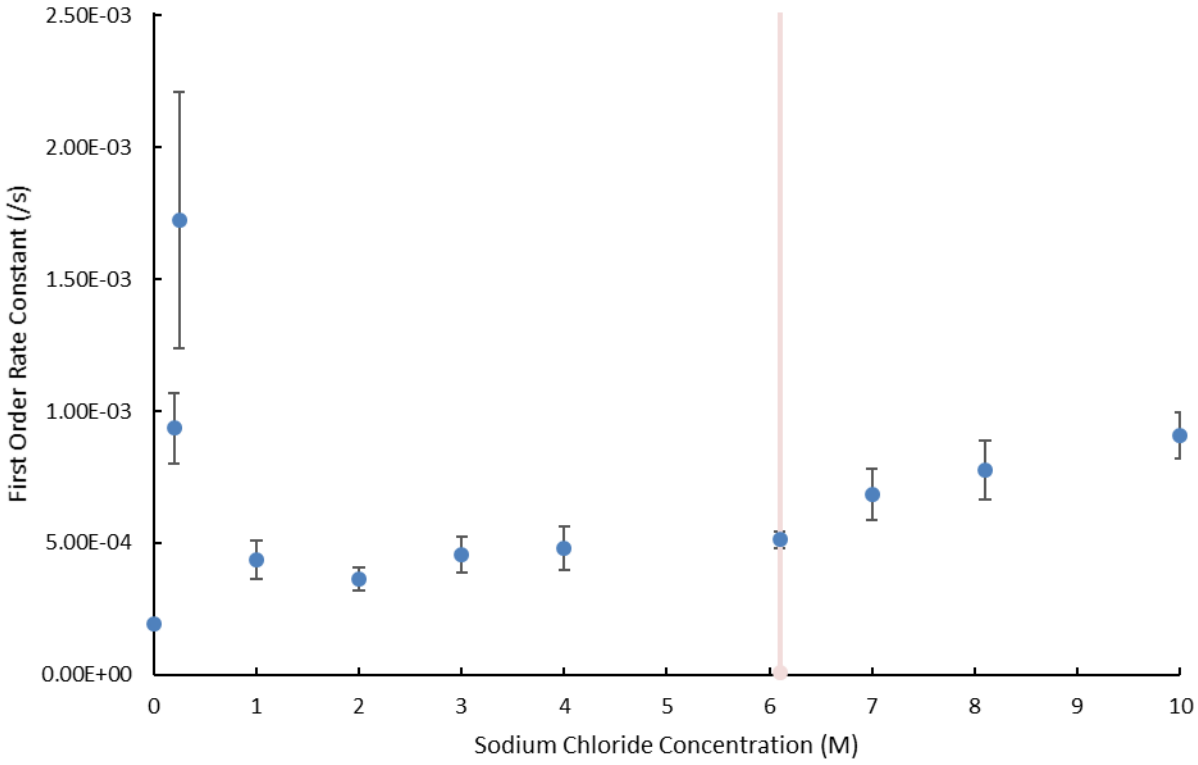

Figure 6: First-order photolysis rate constants for anthracene with increasing sodium chloride concentration. The vertical trace shows sodium chloride's saturation limit in water. Error bars represent the standard deviation of at least three trials.

The increase in rate constant at low sodium chloride concentrations is associated with singlet oxygen production (Grossman et al. in prep). Singlet oxygen is produced in air-saturated waters through the energy transfer of excited organic molecules and molecular oxygen (Glover and Rosario-Ortiz 2013). The presence of halides in solution can enhance intersystem crossing in aromatic species (Glover and Rosario-Ortiz 2013).

At sodium chloride concentrations greater than 0.25 M, the rate constant has a negative dependence on sodium chloride concentration likely due to the quenching of excited anthracene; the quenching is caused by the heavy atom effect, meaning sodium chloride at

these concentrations is promoting excited anthracene into the ground state (Grossman et al. in prep).

While the rate constant drops significantly at sodium chloride concentrations greater than 0.25 M, it never returns to a value as low as that measured in deionized water in the absence of salt. As the salt concentration continues to increase, the rate constant is generally stable between 1 M and 6 M sodium chloride, as seen in Figure 6. The saturation limit for sodium chloride in deionized water is 6.1 M. The rate constant begins to steadily increase beyond the saturation limit, indicating that the saturation of salt in the solution is having some effect on the chemistry. A possible reason for this increase is that the saturated salt in the solution is providing a surface for the anthracene to react on.

Chemistry on particulate surfaces has been studied and photolysis of anthracene has previously been reported to degrade faster when on some surfaces as opposed to dissolved in solution. Anthracene has been shown to photolyze more rapidly on the surface of ice than in liquid water (Kahan and Donaldson 2007). Beyond just anthracene, studies have shown the photolysis of PAHs can be altered greatly when adsorbed to a surface. Acenaphthene at the interface of silica gel and air underwent photochemical degradation faster than in water (Reyes et al. 1998). With these prior studies in mind, a proposal can be made that the increase in photolysis rate between 6.1 M and 10 M sodium chloride, seen in Figure 6, is at least partially due to anthracene adhering to the surface of solid salt in solution and reacting faster photochemically.

While determining what effects the halides could be having on photolysis, an investigation into whether high salt concentrations could be forming anthracene excimers was done. An excimer is a short-lived molecule formed from the combination of two species when a molecule is in an excited state. It has been shown that excimer formation can enable photolysis in benzene and in substituted benzenes, and can potentially change reaction mechanisms (Kahan et al. 2010, Stathis et al. 2016). It has also been shown that excimeric anthracene photolysis progresses more rapidly than monomeric anthracene photolysis (Malley et al. 2017).

Excimeric anthracene might exist at higher sodium chloride concentrations because of the higher local concentration of anthracene (salting out), or because of surface adsorption. Excimeric anthracene has a similar emission spectrum as monomeric anthracene (shown in Figure 5), but the peak centered around 380 nm is absent. Therefore, in the presence of excimers, the peak at 380 nm will be less intense than the peak at 405 nm. Figure 7 shows the ratio of the intensities at 380 nm and 405 nm as a function of salt concentration.

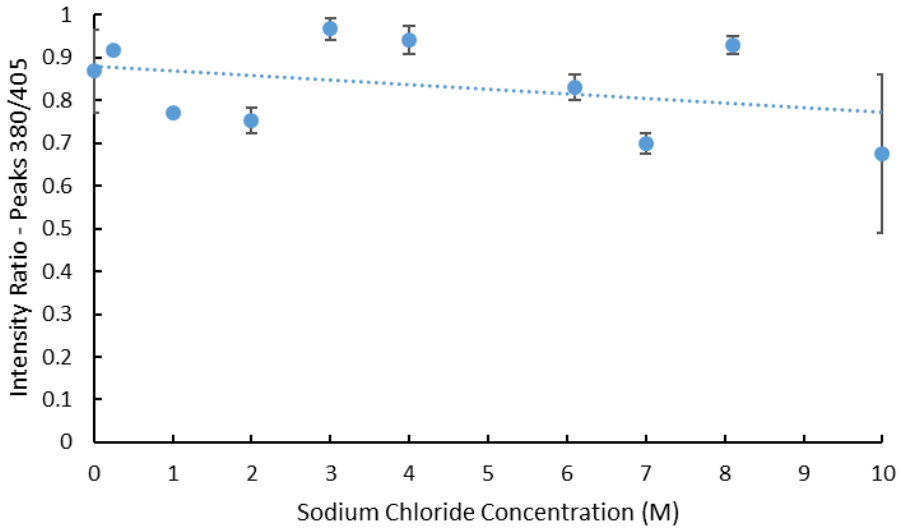

Figure 7: Anthracene intensity ratio of emission peaks 380 nm and 405 nm plotted against sodium chloride concentration for 3×10^{-7} M anthracene in deionized water. Error bars represent the standard deviation of at least three trials.

There is a slight downward trend observed as the salt concentration increases, meaning that the emission peak at 380 nm is decreasing in intensity relative to the peak at 405 nm. However, the change is less than 25% even at sodium chloride concentrations as high as 10 M. This suggests that excimers may not be forming. However, there is also an argument to be made that excimer formation wouldn't be seen even if it was happening. At higher salt concentrations, as the anthracene adheres to the solid salt its fluorescence will be quenched, and the intensity readings will be significantly lower. It is this adsorbed anthracene that would be expected to not show the peak around 380 nm. However, anthracene still in solution would have much higher fluorescence intensity. These higher intensity readings from anthracene in solution may completely overshadow any observable excimer formation.

3.3 - Photolysis in Water vs. Octanol

Octanol, which does not absorb solar photons itself, was used as an organic solvent. Photolysis rates were much slower in octanol solutions. Rate constants obtained from experiments done in octanol were an average of $7.4\times10^{-6} \pm 2\times10^{-7}$ s^{-1}. This is an order of

magnitude slower than those done in water ($1.9\times10^{-4} \pm 1\times10^{-5}$ s^{-1}). The rate constants in octanol agree with rate constants previously reported (Grossman et al. 2016).

It has previously been shown that polarity has a large effect on PAH photolysis kinetics. Octanol is much less polar than water. This difference in polarity can account for significantly reduced rate constants obtained. Past studies have shown that anthracene photolysis kinetics at the air-aqueous interface produced larger rate constants than in less polar solvents (Donaldson and Vaida 2006). There is a direct correlation between polarity and anthracene's photolysis rate constant, which rapidly increases as polarity increases (Grossman et al. 2016).

A similar dependence on sodium chloride concentration was observed in octanol as in water, as seen in Figure 8. The rate constant in the presence of 0.25 M sodium chloride increased by a factor of 2, which is much smaller than the factor of 9 increase observed in water. While the increase in anthracene photolysis rate constant with 0.25 M sodium chloride is less dramatic in octanol than it is in water, it is possible that the enhanced rate constant seen is still due to singlet oxygen production.

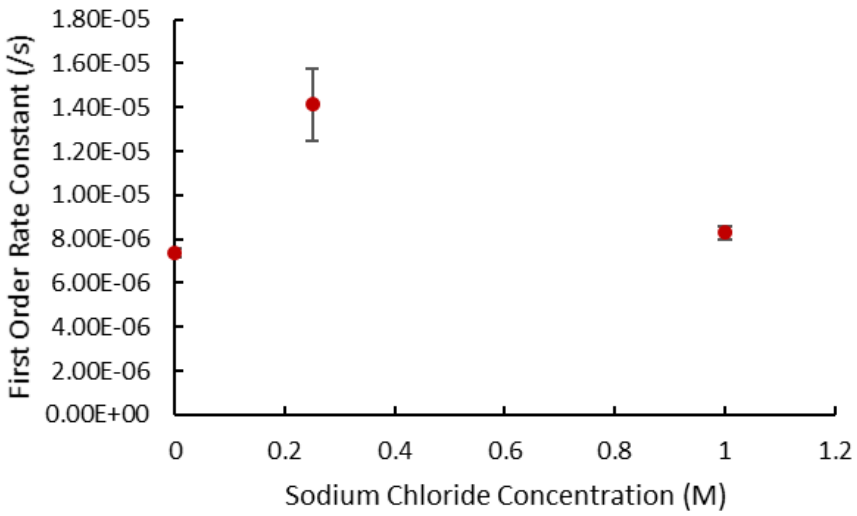

Figure 8: Anthracene photolysis rate constants in octanol as a function of sodium chloride concentration. Error bars represent the standard deviation of at least three trials.

3.4 - Photolysis in Mixed Aqueous-Organic Solution

Photolysis kinetics of anthracene in mixed immiscible aqueous-organic solutions, specifically with deionized water and octanol, have been previously reported (Grossman et al. 2016). In the absence of sodium chloride, we measure rate constants of 1.23×10^{-5} s^{-1} and 4.77×10^{-5} s^{-1} for 90% and 50% octanol solutions respectively, which is in agreement with work previously done in this lab (Grossman et al. 2016).

Figure 9, which shows the rate constant as a function of sodium chloride concentration in 90% and 50% octanol solutions shows the same sodium chloride concentration dependence observed in both water and octanol with a maximum rate constant at 0.25 M sodium chloride. Regardless of the ratio of the aqueous and organic components, the sodium chloride has similar effects on anthracene photolysis kinetics. The only difference is in the degree to which photolysis is enhanced in each solution.

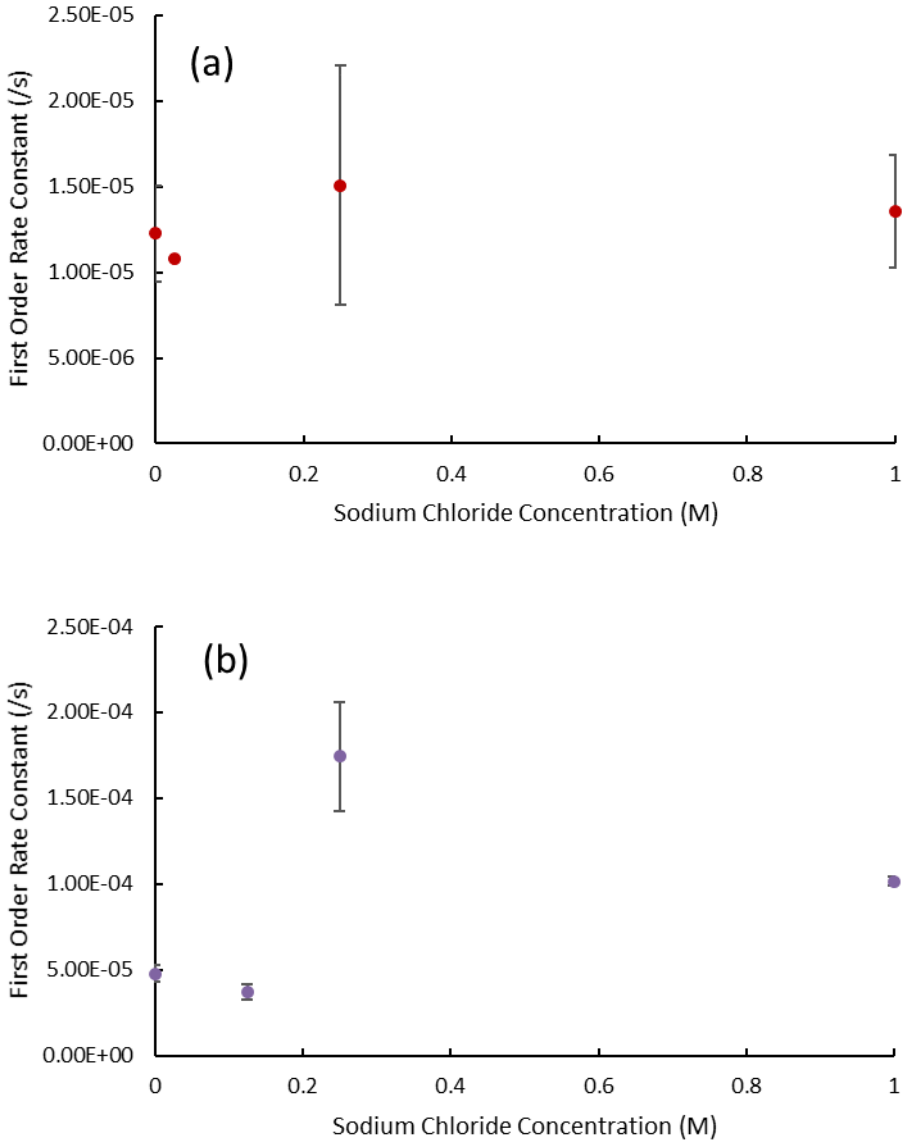

Figure 9: Anthracene photolysis rate constant as a function sodium chloride concentration in (a) 90% octanol and (b) 50% octanol. Error bars represent the standard deviation of at least three trials.

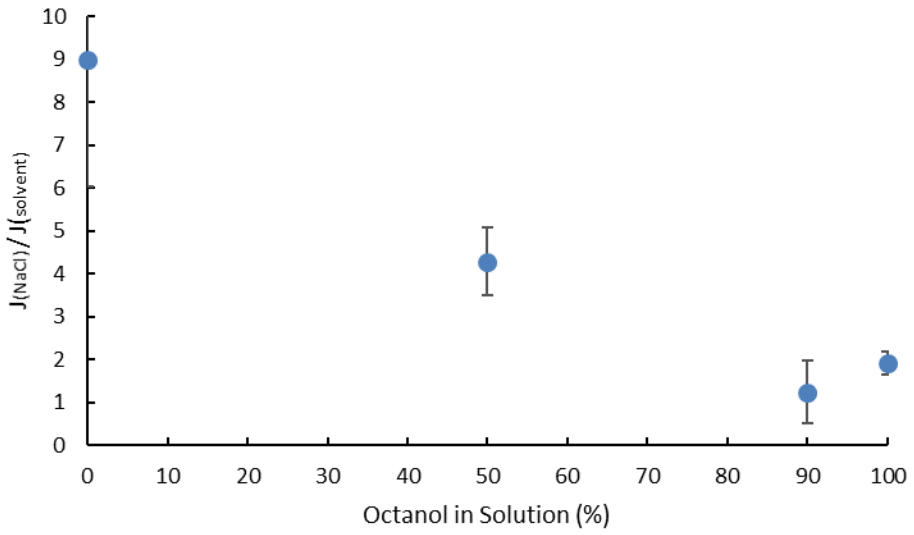

Figure 10: The ratio of the photolysis rate constant (J) in 0.25 M sodium chloride and 0 M sodium chloride for water, 50% octanol, 90% octanol, and octanol between the 0 M and 0.25 M sodium chloride.

Figure 10 shows the change in the rate constants of anthracene photolysis in each solution medium. 90% octanol and 100% octanol solutions were within error of each other, which is to be expected, as previous work done in this lab has shown that solutions as low as 82% octanol were within error of rate constants found in pure octanol (Grossman et al. 2016).

3.5 - Photolysis in Stagnant vs. Turbulent Solution

Atmospheric aerosols may not always achieve equilibrium due to wind action or evaporation. Stirring the solution during photolysis is a way to mimic a disturbed equilibrium. Therefore, work has been done to study the differences in photolysis between actively mixing solutions and solutions at rest. Previous work with mixed immiscible aqueous-organic solutions showed that stirring the solution during photolysis can influence the rate (Grossman et al. 2016). While anthracene normally partitions to the organic phase, a minute amount can partition to the aqueous phase (Asa-Awuku et al. 2009).

Prior work in this lab found that under turbulent conditions, anthracene photolysis was faster than under stagnant conditions suggesting that anthracene continued to partition to the aqueous phase to maintain equilibrium in the total solution. If anthracene no longer partitioned to the aqueous phase after initial phase equilibrium then the difference in anthracene photolysis kinetics in turbulent and stagnant would not be observed until the ratio of water in solution was greater than 99%. As the anthracene in the aqueous phase photodegrades more rapidly, more partitions to the aqueous phase to restore equilibrium (Grossman et al. 2016).

As seen in Figure 11, 90% octanol solution when stirring has higher rate constants than the stagnant counterpart. The 0 M sodium chloride in 90% octanol under turbulent conditions was within error of the stagnant experiments, with rate constants of $1.2\times10^{-5} \pm 3\times10^{-6}$ s^{-1} in the stagnant solution and $8.5\times10^{-6} \pm 1.3\times10^{-6}$ s^{-1} in turbulent solution. Comparatively, Figure 11 shows how the rate constant in 50% octanol solution without any sodium chloride is much higher in the turbulent experiment, in agreement with Grossman et al. The addition of 0.25 M sodium chloride increases anthracene's photolysis rate constants in all samples investigated except turbulent 50% octanol solutions. Under these conditions, photolysis in the presence of 0.25 M sodium chloride is ~37% slower than that in the absence of sodium chloride. The reason for this anomalous behavior will be the subject of future investigations.

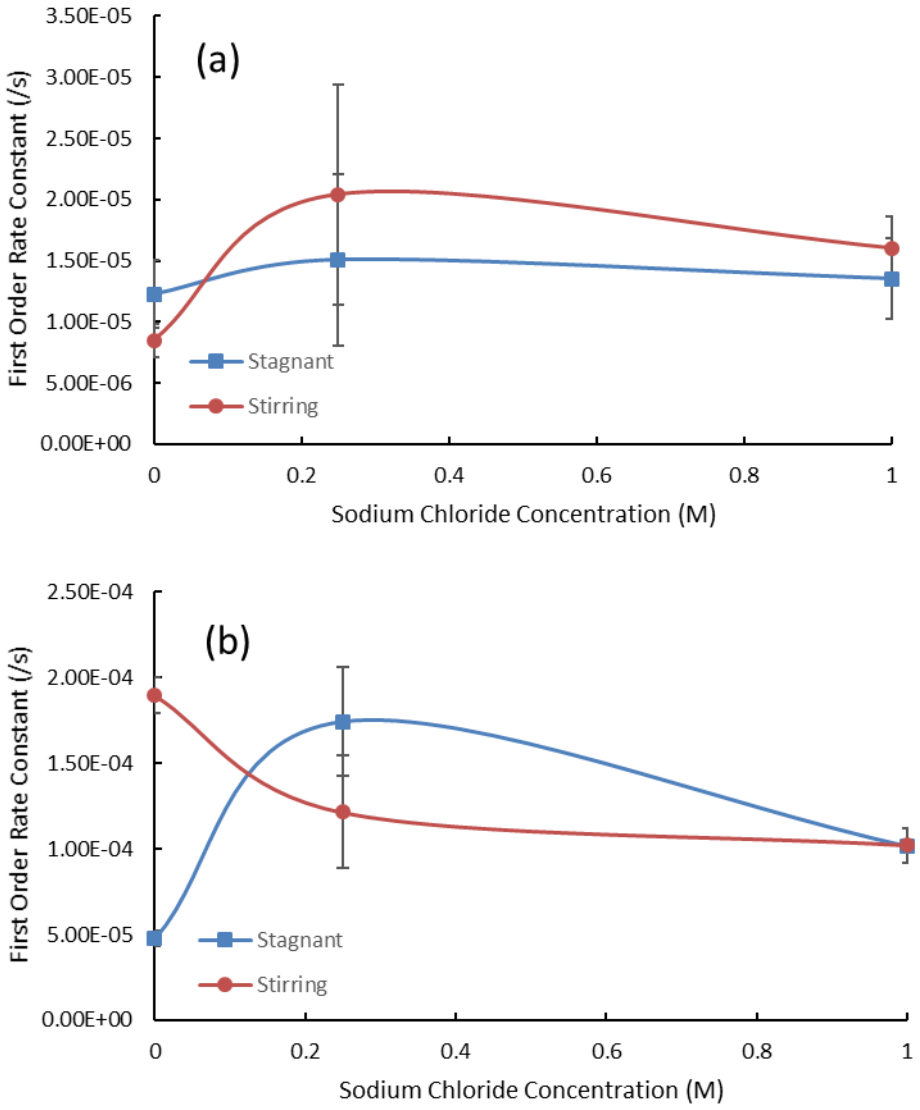

Figure 11: Anthracene photolysis rate constants as a function of sodium chloride concentration in (a) 90% octanol and (b) 50% octanol under stagnant and turbulent conditions. Error bars represent the standard deviation of at least three trials.

3.6 - Effect of Halide Concentration in Mixed Aqueous-Organic Solution

Sodium chloride is much more soluble in water than in octanol. In a mixed aqueous-organic solution, it can be assumed that the sodium chloride partitions preferentially to the aqueous phase of the solution, while PAHs partition to the organic phase (Asa-Awuku et al. 2009). Therefore, the halide and the PAH are expected to be in different phases of the solution,

so anthracene will encounter lower halide concentrations in phase-separated aqueous-organic solutions than in water for the same sodium chloride loading.

The sodium chloride concentrations reported above correspond to the mass dissolved in the total volume of solution. However, local halide concentrations within the aqueous and organic phases are likely quite different. An investigation was done to look at how the rate constant would be affected if the aqueous phase contained 0.25 M sodium chloride. The assumption was that a larger enhancement, more akin to what was seen in the water experiments, would be seen.

The non-linear dependence of sodium chloride concentrations on anthracene photolysis kinetics in water as shown in Figure 5 show that at even a change between 0.20 M and 0.25 M sodium chloride in solution could induce a large change on photolysis rate constants. Assuming the sodium chloride is partitioning completely to the aqueous layer, where it is more soluble, the previous experiments using 0.25 M sodium chloride in total solution would have a higher concentration of sodium chloride in the aqueous phase.

For both the 50% octanol and the 90% octanol solutions, an adjusted 0.25 M sodium chloride solution was made with overall concentrations in the full solution of 0.125 M in 50% octanol and 0.025 M in 90% octanol. When photolysis was done with the adjusted concentrations, it was found that the rates were similar to the rates found in the respective solutions without any sodium chloride as seen in Table 1 and Figure 8.

Table 1: Anthracene photolysis rate constants with no sodium chloride, with low sodium chloride, and high sodium chloride (concentration in total solution: 0.25 M) under stagnant conditions

		J (s^{-1})		
% Octanol	"low [NaCl]" (M)	no NaCl	low NaCl	high NaCl
0	0.25	1.91E-04		1.72E-03
50	0.125	4.77E-05	3.71E-05	2.04E-04
90	0.025	1.23E-05	1.08E-05	1.51E-05

This showed that the effects of sodium chloride on anthracene photolysis kinetics did not strongly depend on the location of sodium chloride in the solution. At sodium chloride concentrations that corresponded to 0.25 M in the aqueous fraction of the solution, rate constants obtained were within error of experiments done with no sodium chloride.

4 - Conclusions

Anthracene photolysis kinetics are affected by changing sodium chloride concentrations in aqueous, organic, and phase-separated solutions. At low concentrations, sodium chloride increases anthracene photolysis due to enhanced production of singlet oxygen (Grossman et al. in prep). In water, at high concentrations below sodium chloride's saturation limit, sodium chloride quenches excited anthracene resulting in lower photolysis rates (Grossman et al. in prep). Beyond sodium chloride's saturation limit, anthracene photolysis kinetics are increased potentially due to anthracene adhering to the surface of solid sodium chloride in solution. There is no notable evidence of excimer formation of anthracene because of higher sodium chloride concentrations, but it could still be happening.

As the fraction of organic solvent in solution increases, anthracene's rate of photolysis decreases. Sodium chloride has similar effects on anthracene photolysis regardless of solution

medium. In mixed aqueous-organic solution, anthracene photolysis kinetics were influenced by sodium chloride concentration in the total solution rather than sodium chloride concentration in the aqueous phase alone.

The evidence that sodium chloride can, in many cases, increase anthracene photolysis kinetics has implications on anthracene in the natural world. It can be proposed that anthracene will degrade faster in sunlight in saline waters than in fresh water. This increased photodegradation will create toxic reaction products at a faster rate, having dangerous implications on human and environmental health.

Appendix

Table 2: Anthracene photolysis kinetic data for all experiments. Rate constant average, standard deviation, excitation wavelength, peak analyzed, and experimental notes.

Anthracene Data									
		Set 1	Set 2	Set 3	Average	Std. Dev.	Excitation λ	Peak Analyzed	Notes
0M NaCl, 1.5E-07M Anthracene	Rate Constant	1.82E-04	2.09E-04	1.83E-04	1.91E-04	1.25E-05	252	380	time interval = 5 min
in water	R^2 value	9.76E-01	9.84E-01	9.96E-01					
0.2M NaCl, 1.5E-07M Anthracene	Rate Constant	9.82E-04	7.53E-04	1.07E-03	9.35E-04	0.000134	252	380	time interval = 2 min
in water	R^2 value	9.78E-01	9.71E-01	9.70E-01					
0.25M NaCl, 3.0E-07M Anthracene	Rate Constant	1.72E-03	1.13E-03	2.32E-03	1.72E-03	4.86E-04	252	381	time interval = 1min
in water	R^2 value	9.97E-01	9.90E-01	2.32E-03					
1M NaCl, 1.5E-07M Anthracene	Rate Constant	5.34E-04	4.22E-04	3.56E-04	4.37E-04	7.35E-05	252	381	time interval = 2min
in water	R^2 value	9.77E-01	9.98E-01	9.69E-01					
2M NaCl, 3.0E-07M Anthracene	Rate Constant	3.11E-04	3.55E-04	4.18E-04	3.61E-04	4.39E-05	252	381	time interval = 3min
in water	R^2 value	8.98E-01	9.53E-01	9.89E-01					
3M NaCl, 1.5E-07M Anthracene	Rate Constant	4.26E-04	3.90E-04	5.49E-04	4.55E-04	6.81E-05	252	381-382	Trial one analyzed at 381, Trial 2+3 analyzed at 382
in water	R^2 value	9.83E-01	9.65E-01	9.79E-01					Slits at 4,4,5,5nm respectively
4M NaCl, 1.5E-07M Anthracene	Rate Constant	4.14E-04	4.33E-04	5.96E-04	4.81E-04	8.17E-05	252	381	Slits at 4,4,5,5nm respectively.
in water	R^2 value	9.75E-01	9.50E-01	9.90E-01					time interval = 3 min
6.1M NaCl, 3.0E-07M Anthracene	Rate Constant	4.68E-04	5.27E-04	5.42E-04	5.12E-04	3.19E-05	252	382	Peak shifted 2nm, signal quenched by salt
in water	R^2 value	9.79E-01	9.97E-01	9.23E-01					time interval = 4 min
7M NaCl, 2.1E-07M Anthracene	Rate Constant	6.85E-04	8.05E-04	5.65E-04	6.85E-04	9.80E-05	252	382	time interval = 2min
in water	R^2 value	9.82E-01	9.61E-01	9.23E-01					slits at 4,4,5,5nm respectively
8.1M NaCl, 3.0E-07M Anthracene	Rate Constant	6.46E-04	7.59E-04	9.23E-04	7.76E-04	0.000114	252	382	Peak shifted 2nm, signal quenched by salt
in water	R^2 value	9.83E-01	9.81E-01	9.92E-01					time interval = 4 min
10M NaCl, 3.0E-07M Anthracene	Rate Constant	8.47E-04	1.03E-03	8.47E-04	9.08E-04	8.63E-05	252	382	Peak shifted 2nm, signal quenched by salt
in water	R^2 value	9.97E-01	9.93E-01	9.94E-01					time interval = 2 min
0M NaCl, 1.0E-07M Anthracene	Rate Constant	7.19E-06	7.25E-06	7.68E-06	7.37E-06	2.18E-07	252	380	time interval = 10min
in Octanol	R^2 value	8.79E-01	8.71E-01	3.94E-01					
0.25M NaCl, 1.0E-07M Anthracene	Rate Constant	1.47E-05	1.58E-05	1.19E-05	1.41E-05	1.64E-06	252	380	time interval = 10min
in Octanol	R^2 value	9.15E-01	6.93E-01	8.03E-01					
1M NaCl, 1.0E-07M Anthracene	Rate Constant	8.64E-06	7.93E-06	8.27E-06	8.28E-06	2.90E-07	252	380	time interval = 10min
in Octanol	R^2 value	7.34E-01	6.95E-01	9.12E-01					
0M NaCl, 1.0E-07M Anthracene	Rate Constant	4.45E-05	4.42E-05	5.43E-05	4.77E-05	4.69E-06	252	380	time interval = 5min
in 50% Octanol	R^2 value	7.86E-01	9.75E-01	9.23E-01					
0.25M NaCl, 1.0E-07M Anthracene	Rate Constant	1.63E-04	2.40E-04	2.09E-04	2.04E-04	3.16E-05	252	380	time interval = 5min
in 50% Octanol	R^2 value	8.47E-01	5.30E-01	9.81E-01					slits at 2,2,4,4nm respectively
1M NaCl, 1.0E-07M Anthracene	Rate Constant	9.92E-05	1.04E-04	9.98E-05	1.01E-04	2.14E-06	252	380	time interval = 5min
in 50% Octanol	R^2 value	4.86E-01	5.79E-01	6.61E-01					slits at 2,2,4,4nm respectively
0M NaCl, 1.0E-07M Anthracene	Rate Constant	2.03E-04	1.78E-04	1.88E-04	1.90E-04	1.03E-05	252	380	time interval = 3min
in 50% Octanol (turbulent)	R^2 value	7.46E-01	6.54E-01	6.86E-01					slits at 2,2,4,4nm respectively
0.25M NaCl, 1.0E-07M Anthracene	Rate Constant	7.60E-05	1.53E-04	1.35E-04	1.21E-04	3.29E-05	252	380	time interval = 3min
in 50% Octanol (turbulent)	R^2 value	8.43E-01	7.33E-01	5.05E-01					slits at 2,2,4,4nm respectively
1M NaCl, 1.0E-07M Anthracene	Rate Constant	1.03E-04	8.94E-05	1.14E-04	1.02E-04	1.01E-05	252	380	time interval = 3min
in 50% Octanol (turbulent)	R^2 value	8.54E-01	7.67E-01	6.04E-01					slits at 2,2,4,4nm respectively
0M NaCl, 1.0E-07M Anthracene	Rate Constant	1.05E-05	1.01E-05	1.62E-05	1.23E-05	2.79E-06	252	380	time interval = 10min
in 90% Octanol	R^2 value	9.29E-01	9.83E-01	6.55E-01					
0.25M NaCl, 1.0E-07M Anthracene	Rate Constant	2.46E-05	8.03E-06	1.26E-05	1.51E-05	6.99E-06	252	380	time interval = 10min
in 90% Octanol	R^2 value	6.29E-01	9.39E-01	6.52E-01					
1M NaCl, 1.0E-07M Anthracene	Rate Constant	1.20E-05	1.81E-05	1.05E-05	1.35E-05	3.29E-06	252	380	time interval = 10min
in 90% Octanol	R^2 value	8.99E-01	9.70E-01	6.67E-01					
0M NaCl, 1.0E-07M Anthracene	Rate Constant	6.83E-06	1.01E-05	8.52E-06	8.48E-06	1.34E-06	252	380	time interval = 15min
in 90% Octanol (turbulent)	R^2 value	9.00E-01	5.14E-01	5.48E-01					
0.25M NaCl, 1.0E-07M Anthracene	Rate Constant	3.17E-05	1.37E-05	1.58E-05	2.04E-05	8.04E-06	252	380	time interval = 5min, 15min
in 90% Octanol (turbulent)	R^2 value	3.74E-01	5.29E-01	9.28E-01					
1M NaCl, 1.0E-07M Anthracene	Rate Constant	1.28E-05	1.93E-05	1.59E-05	1.60E-05	2.65E-06	252	380	time interval = 10min
in 90% Octanol (turbulent)	R^2 value	9.46E-01	9.15E-01	8.94E-01					
0.25M NaCl, 1.0E-07M Anthracene	Rate Constant	3.79E-05	3.16E-05	4.19E-05	3.71E-05	4.24E-06	252	380	time interval = 5min
in 50% Octanol	R^2 value	9.87E-01	8.82E-01	9.78E-01					
0.125M NaCl in aqueous phase									
0.25M NaCl, 1.0E-07M Anthracene	Rate Constant	1.08E-05	1.16E-05	1.01E-05	1.08E-05	6.13E-07	252	380	time interval = 7min
in 90% Octanol	R^2 value	9.29E-01	8.65E-01	8.98E-01					
0.025M NaCl in aqueous phase									

References

Alves, C. A., et al. (2017). "Polycyclic aromatic hydrocarbons and their derivatives (nitro-PAHs, oxygenated PAHs, and azaarenes) in PM2.5 from Southern European cities." Science of the Total Environment **595**: 494-504.

Asa-Awuku, A., et al. (2009). "Mixing and phase partitioning of primary and secondary organic aerosols." Geophysical Research Letters **36**(15): n/a-n/a.

Bostrom, C. E., et al. (2002). "Cancer risk assessment, indicators, and guidelines for polycyclic aromatic hydrocarbons in the ambient air." Environmental Health Perspectives **110**: 451-488.

de Bruyn, W. J., et al. (2012). "Photochemical degradation of phenanthrene as a function of natural water variables modeling freshwater to marine environments." Mar Pollut Bull **64**(3): 532-538.

Donaldson, D. J. and V. Vaida (2006). "The Influence of Organic Films at the Air−Aqueous Boundary on Atmospheric Processes." Chemical Reviews **106**(4): 1445-1461.

EPA (2015). "National Recommended Water Quality Criteria - Human Health Criteria Table."

Fasnacht, M. P. and N. V. Blough (2003). "Mechanisms of the Aqueous Photodegradation of Polycyclic Aromatic Hydrocarbons." Environmental Science & Technology **37**(24): 5767-5772.

Finlayson-Pitts, B. and J. Pitts Jr (2000). "Chemistry of the Upper and Lower Atmosphere." 349-546.

Freedman, M. A., et al. (2010). "Characterizing the Morphology of Organic Aerosols at Ambient Temperature and Pressure." Analytical Chemistry **82**(19): 7965-7972.

George, C., et al. (2015). "Heterogeneous photochemistry in the atmosphere." Chem Rev **115**(10): 4218-4258.

Glover, C. M. and F. L. Rosario-Ortiz (2013). "Impact of Halides on the Photoproduction of Reactive Intermediates from Organic Matter." Environmental Science & Technology **47**(24): 13949-13956.

Grossman, J. N., et al. (in prep). "Anthracene and Pyrene Photolysis Kinetics in Freshwater and Saltwater Environments."

Grossman, J. N., et al. (2016). "Anthracene and pyrene photolysis kinetics in aqueous, organic, and mixed aqueous-organic phases." Atmospheric Environment **128**: 158-164.

Hallquist, M., et al. (2009). "The formation, properties and impact of secondary organic aerosol: current and emerging issues." Atmospheric Chemistry and Physics **9**(14): 5155-5236.

Haritash, A. K. and C. P. Kaushik (2009). "Biodegradation aspects of polycyclic aromatic hydrocarbons (PAHs): a review." J Hazard Mater **169**(1-3): 1-15.

Irwin, R. (1997). "Environmental Contaminants Encylcopedia Anthracene Entry." National Park Service Water Rexources Divisions.

Jacob, D. (1999). "Introduction to Atmospheric Chemistry." Princeton University Press: 144-153.

Jung, K. H., et al. (2014). "Polycyclic aromatic hydrocarbon exposure, obesity and childhood asthma in an urban cohort." Environ Res **128**: 35-41.

Kahan, T. F. and D. J. Donaldson (2007). "Photolysis of Polycyclic Aromatic Hydrocarbons on Water and Ice Surfaces." The Journal of Physical Chemistry A **111**(7): 1277-1285.

Keene, W. C., et al. (2007). "Inorganic chlorine and bromine in coastal New England air during summer." Journal of Geophysical Research **112**(D10).

Larson, S. M. and G. R. Cass (1989). "Characteristics of summer midday low-visibility events in the Los Angeles area." Environmental Science & Technology **23**(3): 281-289.

Malley, P. P. A., et al. (2017). "Effects of Chromophoric Dissolved Organic Matter on Anthracene Photolysis Kinetics in Aqueous Solution and Ice." The Journal of Physical Chemistry A **121**(40): 7619-7626.

May, N. W., et al. (2016). "Lake spray aerosol generation: a method for producing representative particles from freshwater wave breaking." Atmospheric Measurement Techniques **9**(9): 4311-4325.

McConkey, B., et al. (1997). Toxicity of a PAH photooxidation product to the bacteria Photobacterium phosphoreum and the duckweed Lemna gibra: Effects of phenanthrene and its primary photoproduct, phenanthrenequinone.

McDow, S. R., et al. (1996). "An approach to studying the effect of organic composition on atmospheric aerosol photochemistry." Journal of Geophysical Research: Atmospheres **101**(D14): 19593-19600.

Miller, J. S. and D. Olejnik (2001). "Photolysis of polycyclic aromatic hydrocarbons in water." Water Res **35**(1): 233-243.

Pirjola, L., et al. (2017). "Physical and chemical characterization of urban winter-time aerosols by mobile measurements in Helsinki, Finland." Atmospheric Environment **158**: 60-75.

Pszenny, A. A. P., et al. (2004). "Halogen cycling and aerosol pH in the Hawaiian marine boundary layer." Atmospheric Chemistry and Physics **4**(1): 147-168.

Reyes, C., et al. (1998). "Photochemistry of acenaphthene at a silica gel/air interface." Journal of Photochemistry and Photobiology A: Chemistry **112**(2): 277-283.

Shiraiwa, M., et al. (2012). "Hazardous components and health effects of atmospheric aerosol particles: reactive oxygen species, soot, polycyclic aromatic compounds and allergenic proteins." Free Radic Res **46**(8): 927-939.

Simoneit, B. R. T. (2002). "Biomass burning — a review of organic tracers for smoke from incomplete combustion." Applied Geochemistry **17**(3): 129-162.

Spicer, C. W., et al. (1998). "Unexpectedly high concentrations of molecular chlorine in coastal air." Nature **394**: 353.

Turpin, B. J., et al. (2000). "Measuring and simulating particulate organics in the atmosphere: problems and prospects." Atmospheric Environment **34**(18): 2983-3013.

WHO (2015).

Xu, C., et al. (2013). "Photolysis of polycyclic aromatic hydrocarbons on soil surfaces under UV irradiation." Journal of Environmental Sciences **25**(3): 569-575.

Yan, B., et al. (2014). "Source apportionment of polycyclic aromatic hydrocarbons (PAHs) into Central Park Lake, New York City, over a century of deposition." Environ Toxicol Chem **33**(5): 985-992.

Yunker, M. B., et al. (2002). "PAHs in the Fraser River basin: a critical appraisal of PAH ratios as indicators of PAH source and composition." Organic Geochemistry **33**(4): 489-515.

Vita

Kyle Blaha

Phone: (440)-313-7136 109 Concord Place

blahakyle1@gmail.com Syracuse, NY 13210

Education

MS Syracuse University, Environmental Chemistry anticipated 2017
Advisor: Tara Kahan

BA Hiram College, Chemistry May 2015
Minored in History

Honors and Awards

NSF NRT EMPOWER Fellowship 2016

Syracuse University Chemistry Department Third Place Poster Award 2016

Hiram College Heritage Scholarship 2011

Research Experience

Dissertation, Syracuse University, New York 2017
Advisor: Tara Kahan

- Environmental Chemistry
- Effects of Halides on Anthracene Photolysis Kinetics in Aqueous Organic Mixtures

Capstone, Hiram College, Ohio 2015
Advisor: Brian Knettle

- Organic Chemistry
- Solvent and Steric Effects on Aldimine Synthesis

Internship, Hiram College, Ohio 2013
Advisor: Caroline Gray

- Analytical Chemistry
- Analysis of Metal-Ion Concentrations in Soil

Teaching Experience

Teaching Assistant, Hiram College, Ohio 2012-2015

- Co-led Organic Chemistry lab session (2013-15)
- Co-led General Chemistry lab session (2012)

Outreach Volunteer, Akron University, Ohio 2014-2015

- Science Fair judge for Akron Public Schools
- 3-day STEM science fair each spring for grades K-12

Outreach Volunteer, University of Mount Union, Ohio 2014

- Science Fair judge for Ohio District 13 Public Schools
- 1-day STEM science fair for elementary-level students

Skills

- Analytical laboratory techniques, micropipetting, hazardous material handling
- Expertise on Photon Technology International Quantum Master 40 fluorimeter
- Knowledge of Microsoft Excel